

Potential Energy Surfaces for Dissociation Reactions of High-Energy Isomers of N₂O₂

Galina Chaban, Mark S. Gordon,* and Kiet A. Nguyen†

Department of Chemistry, Iowa State University, Ames, Iowa 50011

Received: February 24, 1997; In Final Form: April 7, 1997[⊗]

The kinetic stability with respect to dissociation to two NO molecules was studied for several high-energy isomers of N₂O₂ using multiconfigurational wave functions. All of these isomers are 50–80 kcal/mol higher in energy than 2NO. Three N₂O₂ isomers (a four-membered D_{2h} isomer, a planar C_{2v} isomer, and a bicyclic C_{2v} isomer) are found to be kinetically stable: the estimated barriers to dissociation are about 40 kcal/mol for the D_{2h} isomer and about 20 kcal/mol for each of the other two isomers. Reaction paths for their dissociation were determined using the intrinsic reaction coordinate method and multiconfigurational wave functions.

Introduction

The possible existence of high-energy isomers of NO dimer has been of considerable experimental and theoretical interest recently due to their potential role as new high-energy density materials (HEDM).^{1–6} Stimulated emission pumping experiments of Wodtke and co-workers¹ and studies of photoelectron spectra of N₂O₂[−] by Arnold and Neumark² provide indirect evidence for the existence of several high-energy N₂O₂ species. A number of metastable N₂O₂ isomers have also been predicted recently in theoretical papers.^{4–6} Relative energies of these isomers are in the range 40–80 kcal/mol above the energy of 2NO fragments. However, in order to be useful as high-energy compounds, these species must be kinetically stable; that is, they must be separated from the lower energy isomers and dissociation products by relatively high barriers on the potential energy surfaces.

Besides the adiabatic kinetic stability, the possibility of surface crossings must also be considered, to ensure that there is no lower energy path to products due to nonadiabatic couplings that can decrease the stability of such compounds.⁷ An example is the high-energy asymmetric NNOO isomer.^{5,6} This structure corresponds to a local minimum on the ¹A' potential energy surface and is stable to the spin-allowed decomposition a-N₂O₂ → N₂O(X¹Σ⁺) + O(¹D). However, the minimum-energy crossing point for the singlet and triplet surfaces lies only 2 kcal/mol above the a-N₂O₂ isomer, leading to its predissociation to N₂O(X¹Σ⁺) + O(³P) products.⁵ Consequently, this isomer is not a viable HEDM candidate.

In this paper, we present minimum-energy reaction paths for dissociation of several previously predicted^{4,6} high-energy N₂O₂ species to 2NO fragments, including potential energy barriers separating them and approximate minimum-energy crossing points between nearby singlet and triplet states. We predict that some of the high-energy isomers may be kinetically stable with respect to the N₂O₂ → 2NO dissociation channel.

Theoretical Approach

The N₂O₂ potential energy surfaces have been studied using *ab initio* electronic structure methods employing multiconfigurational self-consistent-field (MCSCF)⁸ wave functions. MCSCF wave functions are necessary for a qualitatively correct description of dissociation processes that involve bond breaking. Two kinds of wave functions were used. One, denoted

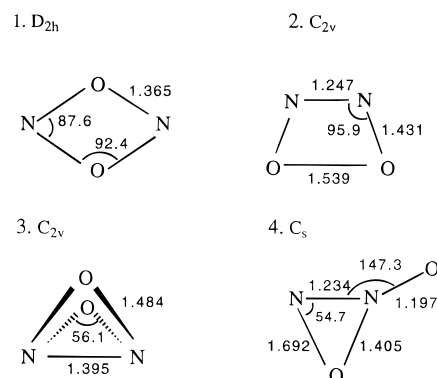


Figure 1. MCSCF(10,10)/6-31G(d) geometric parameters (bond lengths in angstroms, angles in degrees) for N₂O₂ high-energy isomers.

MCSCF(10,10), included all possible configurations, consistent with the appropriate symmetry and spin, that may be obtained by distributing 10 active electrons in 10 active orbitals. Generally speaking, five NO and NN bond orbitals and the five corresponding antibonding orbitals were included in the active space for various isomers. These active orbital choices will be discussed in more detail for each individual isomer. The second active space, MCSCF(14,12), included two oxygen lone pair orbitals (one on each oxygen atom) in addition to the (10,10) space. Inclusion of oxygen lone pairs is necessary to obtain a consistent description of some reactions.

The stationary points on the N₂O₂ potential energy surface have been identified using analytic gradients of MCSCF energies. These stationary points were determined to be minima, transition states, or higher order saddle points by calculating the Hessian (by finite differencing analytic gradients) and verifying that there are 0, 1, or >1 negative eigenvalues, respectively. Minimum-energy paths (MEPs) were determined using the intrinsic reaction coordinate (IRC) method with the second-order algorithm developed by Gonzalez and Schlegel⁹ and a step size of 0.15 amu^{1/2} bohr. Stationary point searches and IRC calculations were performed using MCSCF(10,10) and MCSCF(14,12) wave functions and the 6-31G(d)¹⁰ basis set. These calculations were done using the GAMESS¹¹ electronic structure program.

The energies of stationary points, as well as selected points along the MEPs, were recalculated with the multiconfigurational second-order perturbation theory method (CASPT2¹²) to account for dynamic correlation. The CASPT2 wave functions were based on MCSCF(10,10) (denoted as CASPT2(10,10)) and MCSCF(14,12) (denoted as CASPT2(14,12)) reference wave

† Current address: Department of Chemistry, University of Alabama, Birmingham, AL.

[⊗] Abstract published in *Advance ACS Abstracts*, May 15, 1997.

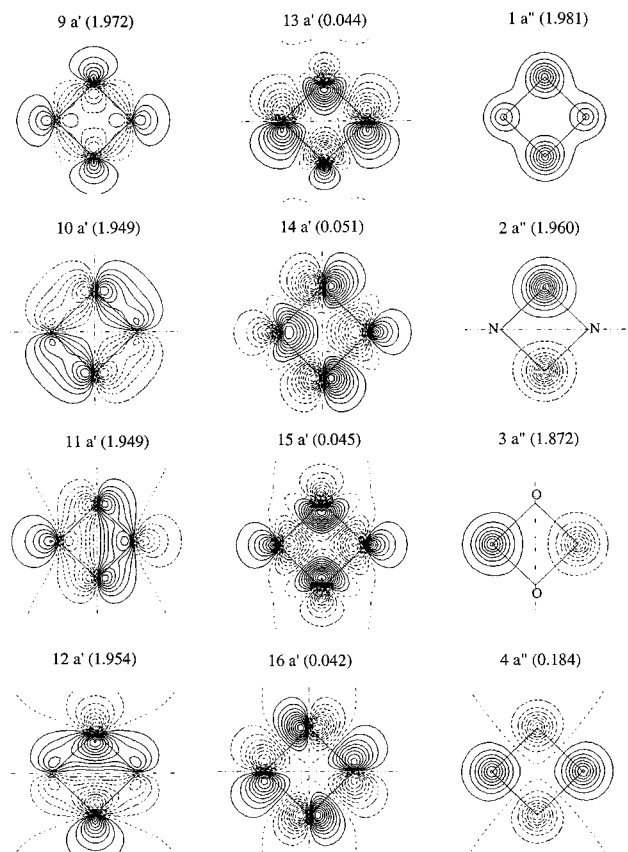


Figure 2. MCSCF(14,12)/6-31G(d) natural orbitals for isomer **1**. a' orbitals are given in the x - y plane; a'' orbitals are given in the plane shifted by 0.2 Å parallel to the x - y plane.

functions with 6-31G(d) and 6-311+G(2d)¹³ basis sets. These calculations were performed using the MOLCAS¹⁴ program. The effect of basis set improvement on the relative energies is small, with corrections on the order of 2–4 kcal/mol. On the other

hand, the addition of dynamic correlation via CASPT2 has a much larger effect, with corrections ranging from 8 to 23 kcal/mol.

Results and Discussion

The four high-energy singlet isomers of N_2O_2 considered in this paper are shown in Figure 1, with the structural parameters obtained at the MCSCF(10,10)/6-31G(d) level of theory. The structure and energetics of isomers **1–3** have been studied previously⁴ at several levels of theory including the MCSCF(10,10) and CASPT2(10,10) levels used in this paper. The Hartree–Fock and MP2/6-31+G(d) structures for isomer **4** have been reported by Arnold and Neumark.² All four isomers are relatively high in energy: planar isomers **1**, **2**, and **4** are about 50 kcal/mol higher than 2NO, and the bicyclic isomer **3** is about 80 kcal/mol above the energy of 2NO. Here we consider the kinetic stability for each of these isomers with respect to dissociation to two NO molecules.

Dissociation of D_{2h} Cyclic Isomer 1. Isomer **1** in Figure 1 has a planar ring structure with four equal N–O bonds (D_{2h} symmetry). This isomer was first reported by Chaban, Klimenko, and Charkin.¹⁵ The detailed electronic structure of this isomer is described in ref 4. The smaller MCSCF(10,10) active space used to study this isomer includes four $\sigma(N-O)$ bonds, four corresponding $\sigma^*(N-O)$ antibonding orbitals, and the $\pi(N-N)$ and $\pi^*(N-N)$ orbitals. An expanded (14 electron, 12 orbital) active space includes additional electrons and orbitals that correspond to the lone pair on each oxygen that interacts with the π space. The MCSCF(14,12) natural orbitals and their occupation numbers are shown in Figure 2. Orbital labels are given using C_s symmetry notations in order to have the same orbital labels for the entire dissociation reaction path. There is significant configurational mixing in this isomer, with 0.366 electrons occupying orbitals that are empty at the single configuration level of theory. The D_{2h} isomer is 50 kcal/mol higher in energy than 2NO molecules at the CASPT2(14,12)/6-311+G(2d) level of theory. This energy is overestimated at

	minimum	transition state	dissociation products
MCSCF(10,10)/6-31G(d) geometries, Å, deg.			2 NO
Relative energies, kcal/mol			
MCSCF(10,10)/6-31G(d)	0.0	50.9	-71.0
CASPT2(10,10)/6-31G(d)	0.0	54.3	-49.0
CASPT2(10,10)/6-311+G(2d)	0.0	52.2	-48.7
MCSCF(14,12)/6-31G(d) geometries, Å, deg.			2 NO
Relative energies, kcal/mol			
MCSCF(14,12)/6-31G(d)	0.0	47.5	-68.7
CASPT2(14,12)/6-31G(d)	0.0	41.5	-48.4
CASPT2(14,12)/6-311+G(2d)	0.0	39.4	-49.8

Figure 3. Structure and energetics for the D_{2h} cyclic isomer (**1**) and the transition state for its decomposition to two NO molecules.

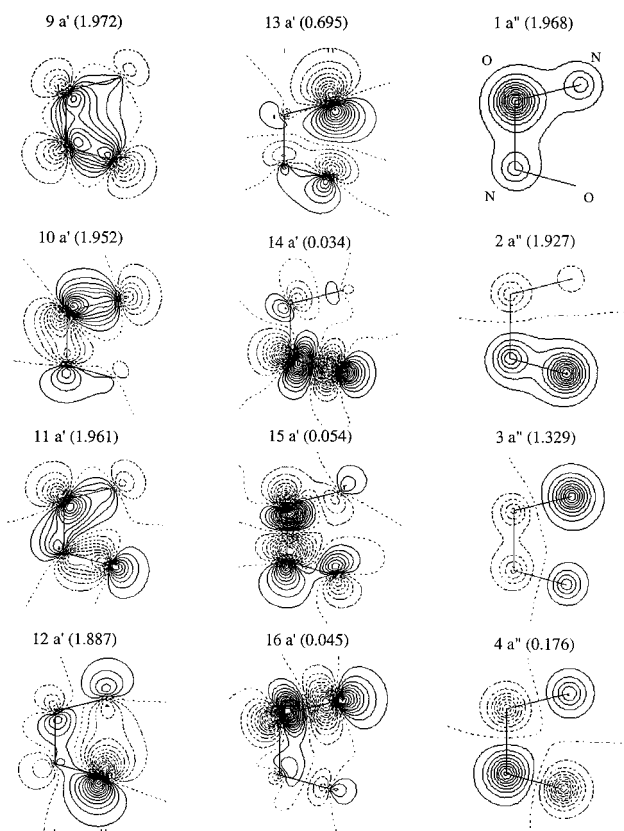


Figure 4. MCSCF(14,12)/6-31G(d) natural orbitals for the transition state for dissociation of isomer **1**. *a'* orbitals are given in the *x-y* plane; *a''* orbitals are given in the plane shifted by 0.2 Å parallel to the *x-y* plane.

the MCSCF level by about 20 kcal/mol. The effect of the active space on the dissociation exothermicity is very small.

The transition state for decomposition of **1** to 2NO and the associated energetics are shown in Figure 3. The transition state geometry is predicted to have *C_s* symmetry. Both active spaces predict considerable asymmetry in the transition state structure, although there are significant differences in the structural details. For example, the longest N–O distance shortens by nearly 0.4 Å upon going from the MCSCF(10,10) to the MCSCF(14,12) level. MCSCF(14,12)/6-31G(d) natural orbitals for the transition state structure are shown in Figure 4. Note that the antibonding σ^* orbital corresponding to the partially broken N–O bond (13 *a'*) has a significant occupation number of 0.695 electrons. Indeed, the set of virtual orbitals that would be empty in the Hartree–Fock wave function contain slightly more than one electron at this MCSCF(14,12) transition state structure. The effect of the expanded active space on the MCSCF barrier height is rather small (only 3 kcal/mol), but when dynamic correlation is included at the CASPT2 level, the barrier height decreases quite significantly: from 52 to 39 kcal/mol. This is probably due to significant changes in the geometry of the transition state upon going from the MCSCF(10,10) to the MCSCF(14,12) level.

Energetics along the dissociation path **1** → 2NO are presented in Figure 5. Although the MCSCF(10,10) active space is sufficient for a description of the *D_{2h}* isomer structure and the net energetics of its dissociation to 2NO, the incorporation of the two oxygen lone pairs is essential to obtain a smoothly varying wave function along the reaction path that connects this isomer with 2NO. This is shown in Figure 5a, where small black circles correspond to the minimum-energy path (MEP)

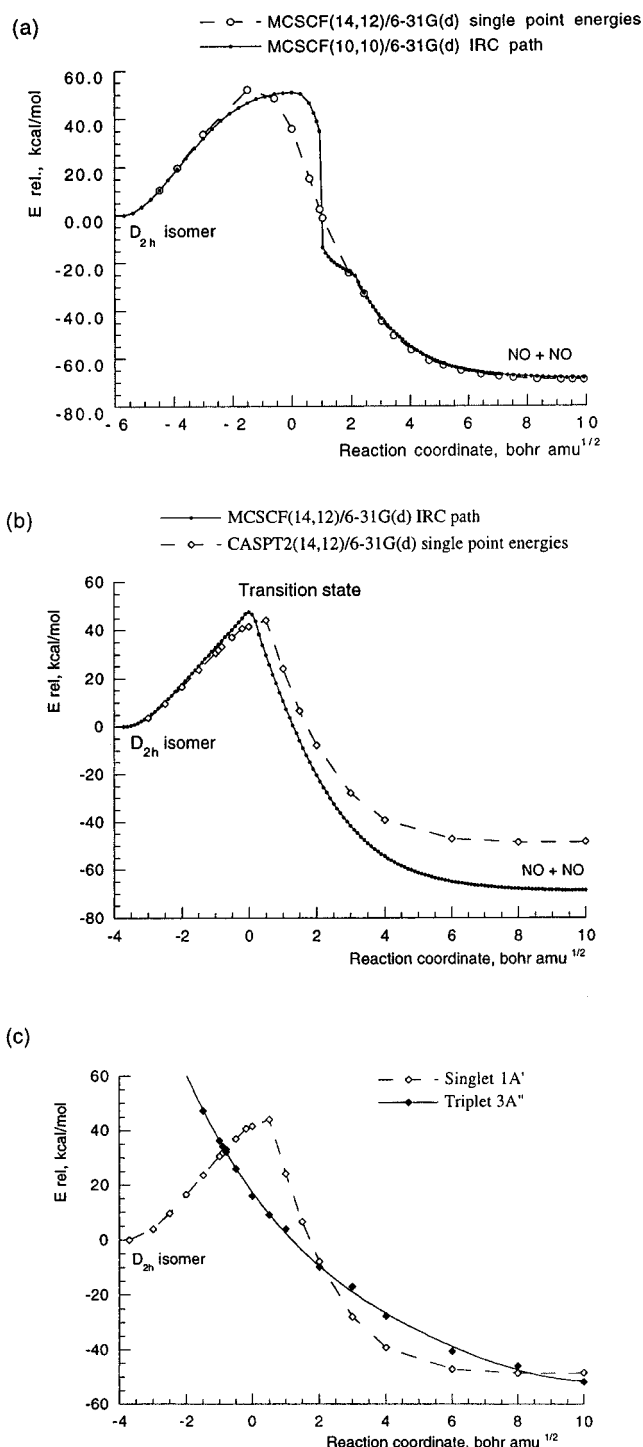


Figure 5. Reaction path for decomposition of *D_{2h}* isomer (**1**) to 2NO: (a) MCSCF(10,10)/6-31G(d) IRC path and MCSCF(14,12)/6-31G(d) single-point energies (open circles); (b) MCSCF(14,12)/6-31G(d) reaction path and CASPT2(14,12)/6-31G(d) single-point energies; (c) CASPT2(14,12)/6-31G(d) energies for singlet (¹A') and triplet (³A'') states along the dissociation reaction path.

for this reaction at the MCSCF(10,10)/6-31G(d) level of theory, and open circles correspond to single-point MCSCF(14,12)/6-31G(d) energies at the MCSCF(10,10) geometries. The MCSCF(10,10) transition state connects smoothly to the *D_{2h}* isomer, but the part of the IRC connecting the transition state to 2NO has a discontinuity due to a change in the active space orbitals. This discontinuity reflects the incompleteness of the (10,10) active space: the active space after the discontinuity contains 6 *a'* and 4 *a''* orbitals while the original active space has 8 *a'* and 2 *a''* orbitals. Inclusion of the two oxygen lone pairs with

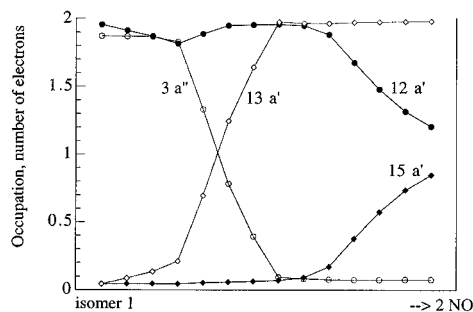


Figure 6. MCSCF(14,12) natural orbital occupation numbers along the dissociation **1** \rightarrow 2 NO.

a'' symmetry provides a complete active space ($8 a' + 4 a''$) that can be used consistently along the entire reaction path. Although computation of such a wave function is very time-consuming (it includes 85 212 configurations vs 9996 configurations for the (10,10) space), it is necessary to obtain a correct IRC.

The resulting MCSCF(14,12) minimum-energy path is shown in Figure 5b. The barrier height for this reaction is about 40 kcal/mol at the best, CASPT2(14,12)/6-311+G(2d), level used here. Changes in the MCSCF natural orbital occupation numbers along this reaction path are shown in Figure 6 for the $12 a'$, $13 a'$, $15 a'$, and $3 a''$ orbitals. $12 a'$ and $15 a'$, almost doubly occupied and empty, respectively, at the isomer **1** geometry, become two singly occupied $\pi^*(\text{N}-\text{O})$ orbitals at the dissociation limit. In addition to this, the almost doubly occupied $3 a''$ orbital becomes empty upon dissociation, while $13 a'$ changes its occupation from 0 to 2. Therefore, this reaction is Woodward–Hoffmann forbidden, and this leads to the high reaction barrier.

Figure 5c illustrates the CASPT2(14,12)/6-31G(d) energies for the lowest singlet ($^1A'$) and triplet ($^3A''$) states at selected geometries along the ground singlet state MEP. The repulsive $^3A''$ state crosses the singlet before the transition state (that is, on the reactant side), but this crossing is predicted to occur at an energy that is about 32 kcal/mol above the reactant well.

So, it is likely that singlet–triplet interaction will not destroy the stability of isomer **1**.

We conclude that the D_{2h} isomer is kinetically stable with respect to dissociation to two NO molecules. Other possible dissociation channels (for example, to $\text{N}_2 + \text{O}_2$) are likely to contain even higher potential energy barriers since considerably more electronic and geometric rearrangements would be involved; therefore, this isomer should be considered to be a possible candidate for isolation and use as a source of energy.

Dissociation of C_{2v} Planar Cyclic Isomer 2. MCSCF(10,10) and MCSCF(14,12) structures and energetics for planar cyclic isomer **2** and the transition state for its decomposition into 2NO are shown in Figure 7. Isomer **2** is also quite high in energy, about 45 kcal/mol above the two NO fragments at the highest level of theory. This isomer has an $\text{N}=\text{N}$ double bond, two single $\text{N}-\text{O}$ bonds, and a single $\text{O}-\text{O}$ bond. The (10,10) active space includes these four σ and one π bond, as well as the corresponding antibonding orbitals. As in the case of isomer **1**, the (14,12) space includes two additional filled π orbitals, one from each oxygen atom. The transition state structure is not planar; it is twisted by about 15° (due to the broken $\text{O}-\text{O}$ bond) and has no symmetry (although it is very close to C_2). The structural parameters obtained using the two MCSCF active spaces are quite similar.

In C_1 symmetry, the MCSCF(14,12) wave function includes 169 884 configurations, so IRC calculations at this level are extremely expensive. The reaction path in this case was followed only at the MCSCF(10,10) level (19 404 configuration wave function). This reaction path is shown in Figure 8. Also shown are CASPT2 single-point energies for singlet and triplet states calculated at several points along the IRC path. The height of the barrier is estimated to be about 19 kcal/mol. There is little variation among the various levels of theory. The reaction proceeds by breaking the $\text{O}-\text{O}$ bond first and then breaking the $\text{N}-\text{N}$ bond.

The lowest triplet state is higher in energy than the singlet state for all points along the reaction path at the CASPT2(10,10)

	minimum	transition state	dissociation products
	C_{2v}	C_1	
			2 NO
MCSCF(10,10)/6-31G(d) geometries, Å, deg.			
<u>E rel. kcal/mol</u>			
MCSCF(10,10)/6-31G(d)	0.0	19.8	-41.6
CASPT2(10,10)/6-31G(d)	0.0	19.6	-47.7
MCSCF(10,10)/6-311+G(2d)	0.0	20.2	-47.0
CASPT2(10,10)/6-311+G(2d)	0.0	20.5	-53.1
	C_{2v}	C_1	
			2 NO
MCSCF(14,12)/6-31G(d) geometries, Å, deg.			
<u>E rel. kcal/mol</u>			
MCSCF(14,12)/6-31G(d)	0.0	22.6	-62.3
CASPT2(14,12)/6-31G(d)	0.0	18.7	-44.2
MCSCF(14,12)/6-311+G(2d)	0.0	22.5	-60.6
CASPT2(14,12)/6-311+G(2d)	0.0	18.7	-44.9

Figure 7. Structure and energetics for C_{2v} planar isomer (**2**) and the transition state for its decomposition to two NO molecules.

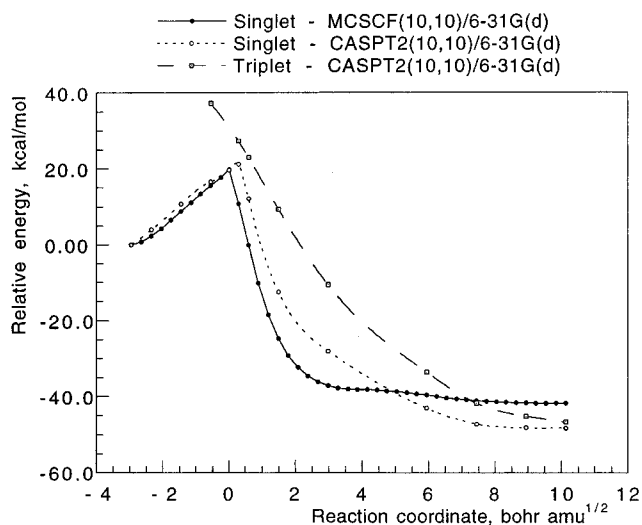


Figure 8. MCSCF(10,10)/6-31G(d) reaction path for decomposition of C_{2v} isomer (**2**) to two NO molecules.

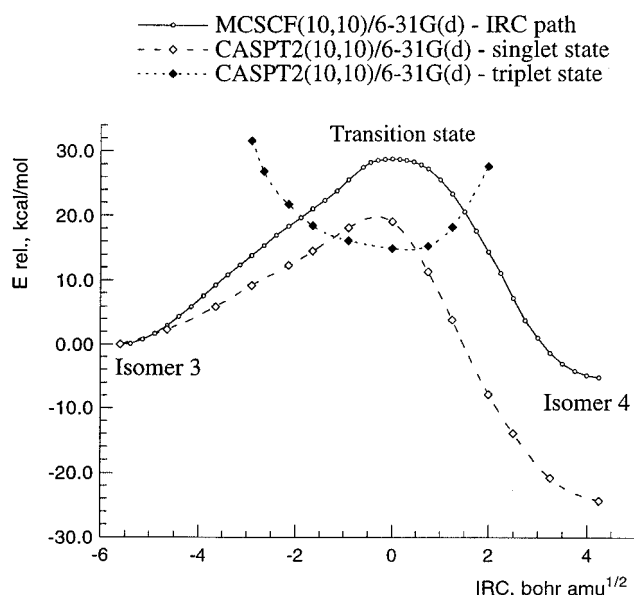


Figure 9. MCSCF(10,10)/6-31G(d) reaction path for isomerization **3** → **4**.

level of theory (Figure 8). When the single-point energies are calculated using the larger MCSCF(14,12) active space (along the same MCSCF(10,10) reaction path), the CASPT2(14,12) triplet is found to be 4 kcal/mol lower than the corresponding

singlet, at the transition state geometry. Although the triplet state is close to the singlet in energy in the transition state region, the triplet energy is much higher in the reactant channel. Again, it is unlikely that the singlet–triplet crossing will prevent detection of isomer **2**. More careful calculations in the singlet–triplet crossing region, including determination of the nonadiabatic interactions,⁷ are, of course, desirable.

Stability of Bicyclic Isomer 3. Bicyclic isomer **3** (Figure 1) is one of the highest isomers on the N₂O₂ potential energy surface: its relative energy with respect to 2NO is about 82 kcal/mol. It has a strained structure of two three-membered N–O–N rings with an O–N–N–O dihedral angle equal to 107°. The MCSCF active space (10,10) used to describe **3** included the N–N and four N–O bonding orbitals and the five corresponding antibonding orbitals. This isomer, as well as the part of the potential energy surface connecting this isomer with the planar ring **1**, was studied in detail previously.⁶ The two isomers were found to be separated by a barrier of 40 kcal/mol. Therefore, the stability of the bicyclic isomer with respect to isomerization to **1** was established.

In an attempt to find a reaction path leading to the dissociation of the isomer **3**, we found that breaking one of the N–O bonds leads to a transition state connecting this isomer to another planar isomer **4**. The dissociation to two NO molecules occurs here in two steps: first, **3** isomerizes to **4** through a barrier of about 20 kcal/mol, and then, isomer **4** dissociates to 2NO with a rather small barrier of about 7 kcal/mol.

The MCSCF(10,10)/6-31G(d) IRC path for the first (isomerization) part of the potential energy surface is shown in Figure 9. The structures of the isomers **3** and **4**, and the structure of the isomerization transition state, as well as their relative energies, are shown in Figure 10. When dynamic correlation (CASPT2) is included, isomer **4** is predicted to be 26 kcal/mol lower in energy than **3**, and the **3** → **4** barrier height is 19 kcal/mol. The lowest triplet state is about 4 kcal/mol lower than singlet at the transition state geometry and is much higher in energy for both isomers (see Figure 9). Therefore, the bicyclic isomer **3** is probably kinetically stable with respect to rearrangement to isomer **4**, although the barrier for this channel is lower than for the rearrangement **3** → **1**. Breaking one of the N–O bonds of **3** leads to rearrangement to isomer **4**, and breaking of the N–N bond leads to **1**. Since both processes involve substantial barriers, the bicyclic isomer may be a good candidate for a metastable high-energy species. Its isolation, however, may be difficult because very high energy (at least 100 kcal/mol) has to be provided to 2NO to overcome the lowest barrier leading to this isomer.

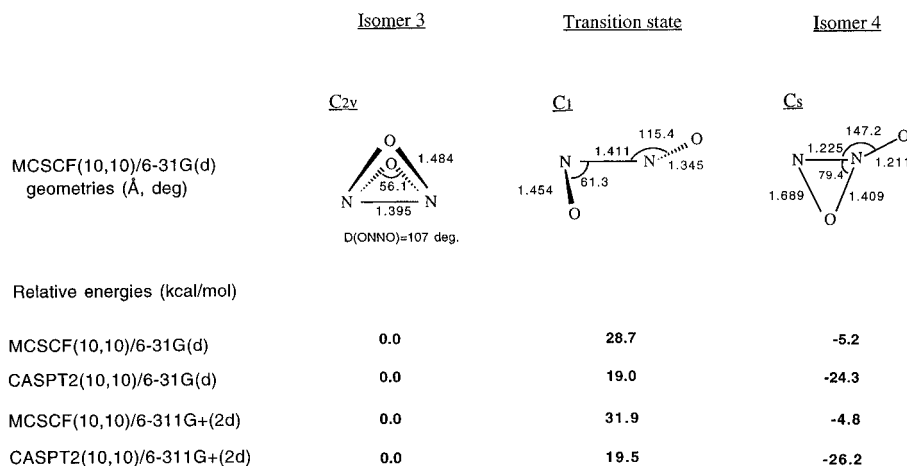


Figure 10. MCSCF(10,10)/6-31G(d) geometries and relative energies for the N₂O₂ isomers **3** and **4** and the transition state for **3** → **4** isomerization.

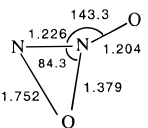
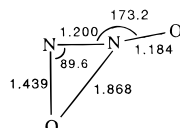
	Isomer 4	Transition state	Dissociation products
	C_s	C_s	2 NO
MCSCF(14,12)/6-31G(d) geometries (Å, deg)			
Relative energies (kcal/mol)			
MCSCF(14,12)/6-31G(d)	0.0	12.3	-80.7
CASPT2(14,12)/6-31G(d)	0.0	7.8	-51.8
CASPT2(14,12)/6-311G+(2d)	0.0	7.3	-48.5

Figure 11. MCSCF(14,12)/6-31G(d) structure and relative energies for the isomer 4 and the transition state for its dissociation to 2NO.

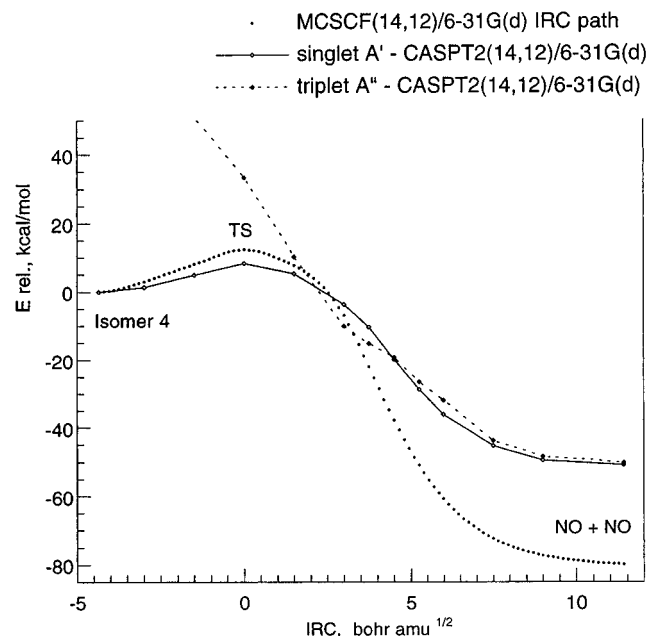


Figure 12. MCSCF(14,12)/6-31G(d) reaction path for decomposition of isomer 4 to two NO molecules.

Dissociation of C_s Planar Isomer 4. MCSCF(10,10) and MCSCF(14,12) structures of the isomer 4 are shown in Figures 10 and 11, respectively. This isomer has short (almost double) N–N (1.23 Å) and N–O (1.20 Å) bonds, one single N–O bond (1.4 Å), and one very weak N–O bond (1.7 Å). Our MCSCF structural parameters are close to those found at the MP2/6-31+G(d) level by Arnold and Neumark.² This isomer is about 48.5 kcal/mol higher in energy than 2NO at the highest, CASPT2(14,12)/6-31+G(2d), level of theory (Figure 11).

The dissociation reaction $4 \rightarrow 2\text{NO}$ was studied at the MCSCF(14,12)/6-31G(d) level of theory. The corresponding reaction path is shown in Figure 12, along with single-point CASPT2 energies for both the lowest singlet and triplet states obtained at several selected points on the MCSCF(14,12) IRC path. The transition state for this process is shown in Figure 11. Its structure shows that the first stage of the dissociation process involves transfer of the (single bond) oxygen atom from one nitrogen atom to another. This requires only a small amount of energy, resulting in a barrier height of about 7 kcal/mol (CASPT2). The MCSCF active orbitals at the transition state structure are shown in Figure 13. During the second part of this reaction, the N–N bond breaks, with the $\pi(\text{N–N})$ and $\pi^*(\text{N–N})$ orbitals (3 a' and 4 a'') rearranging into two singly occupied $\pi^*(\text{N–O})$ orbitals of the dissociation products (Figure 14).

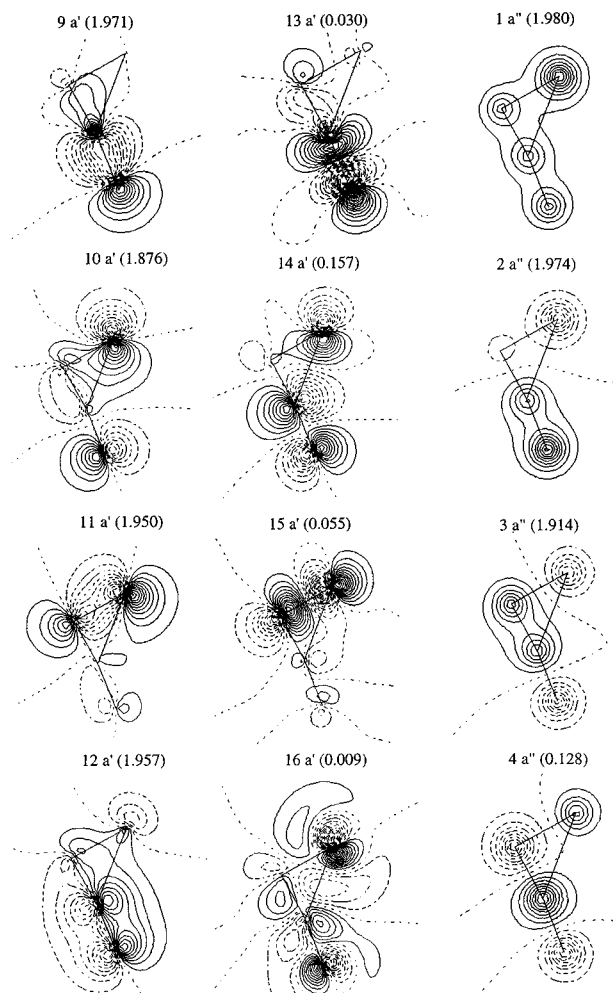


Figure 13. MCSCF(14,12)/6-31G(d) natural orbitals for the transition state for dissociation of isomer 4. a' orbitals are given in the x - y plane; a'' orbitals are given in the plane shifted by 0.2 Å parallel to the x - y plane.

The triplet ($^3A''$) state is higher in energy than the singlet in the region of the minimum and transition state and becomes close to the singlet state in the product (2NO) part of the reaction (Figure 12). The small barrier for this reaction suggests that structure 4 may be stable only at low temperatures. On the other hand, this isomer has the lowest barrier for the reverse reaction, $2\text{NO} \rightarrow$ isomer 4, and may be responsible for the enhanced vibrational relaxation observed by Wodtke and co-workers¹ for excitation energies above vibrational quantum number $v \approx 12$. The barrier height is about 56 kcal/mol (2.4 eV), which is in the region where vibrational relaxation accelerates.¹ Two NO molecules at large separation, with one

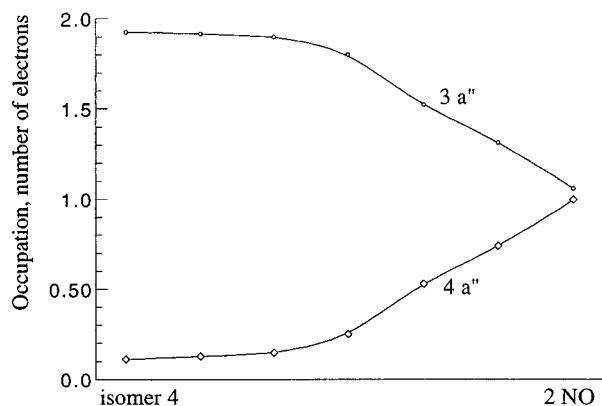


Figure 14. MCSCF(14,12) natural orbital occupation numbers along the dissociation **4** \rightarrow 2NO.

in its ground vibrational state and the other with the N–O bond stretched to 1.55 Å (corresponding to $v \approx 15$), have an energy that is about 4 kcal/mol above the 2NO \rightarrow **4** reaction barrier height. This supports the suggestion made in ref 1 that the trajectory for collision NO($v=0$) + NO($v \geq 12$) may pass near the transition state for formation of isomer **4** or other high-energy isomers.

Conclusion

Dissociation and isomerization reactions were studied for four high-energy isomers of N₂O₂ in order to determine their kinetic stability. The isomers included the four-membered ring D_{2h} isomer (**1**), the planar C_{2v} isomer (**2**), the bicyclic C_{2v} isomer (**3**), and the planar C_s isomer (**4**) shown in Figure 1. Minimum-energy reaction paths have been determined using IRC techniques and MCSCF(10,10) and MCSCF(14,12) wave functions. Potential energy barriers separating the isomers from 2NO products and approximate minimum-energy crossing points between closest singlet and triplet states were determined. The energetics for these reactions were calculated using second-order perturbation theory based on MCSCF wave functions (CASPT2).

We predict that isomers **1** and **2** may be kinetically stable with respect to dissociation to two NO molecules: the predicted barrier heights to dissociation are about 40 kcal/mol for the D_{2h} isomer and about 20 kcal/mol for the planar C_{2v} ring. Low-lying triplet states are found to cross the singlet potential energy surfaces along the reaction paths for these two isomers, but these crossings occur in regions that are far enough from the positions of the minima that they are unlikely to destroy the stability of these isomers.

The bicyclic isomer **3** is found to isomerize to isomer **4** via a barrier of about 19 kcal/mol. In turn, the isomer **4** dissociates to 2NO via a small barrier of about 7 kcal/mol and is probably unstable.

We suggest that isomers **1**, **2**, and **3** may be good candidates for high-energy systems and that experimental attempts should be made to synthesize them.

Acknowledgment. This work was supported by the Air Force Office of Scientific Research (grant F49620-95-1-0077). The calculations were performed in part on the IBM SP2 at the Maui Supercomputer Center, in part on a local eight node SP2 obtained with funds provided by the National Science Foundation, the Air Force Office of Scientific Research, and Iowa State University, and in part on IBM and DEC workstations provided by the same funding sources. The authors thank Prof. A. Wodtke for useful suggestions regarding the manuscript.

References and Notes

- (1) (a) Yang, X.; Kim, E. H.; Wodtke, A. M. *J. Chem. Phys.* **1992**, *96*, 5111. (b) Yang, X.; Price, J. M.; Mack, J. A.; Morgan, C. G.; Rogaski, C. A.; McGuire, D.; Kim, E. H.; Wodtke, A. M. *J. Phys. Chem.* **1993**, *97*, 3944.
- (2) Arnold, D. W.; Neumark, D. M. *J. Chem. Phys.* **1995**, *102*, 7035.
- (3) Michels, H. H.; Montgomery, J. A. *J. Chem. Phys.* **1988**, *88*, 7248.
- (4) Nguyen, K. A.; Gordon, M. S.; Montgomery, J. A.; Michels, H. H. *J. Phys. Chem.* **1994**, *98*, 10072.
- (5) Nguyen, K. A.; Gordon, M. S.; Montgomery, J. A.; Michels, H. H.; Yarkony, D. R. *J. Chem. Phys.* **1994**, *98*, 3845.
- (6) Nguyen, K. A.; Gordon, M. S.; Boatz, J. A. *J. Am. Chem. Soc.* **1994**, *116*, 9241.
- (7) (a) Yarkony, D. R. *J. Am. Chem. Soc.* **1992**, *114*, 5406. (b) Yarkony, D. R. *J. Chem. Phys.* **1990**, *92*, 2457.
- (8) (a) Ruedenberg, K.; Schmidt, M. W.; Gilbert, M. M.; Elbert, S. T. *J. Chem. Phys.* **1982**, *71*, 41. (b) Lam, B.; Schmidt, M. W.; Ruedenberg, K. *J. Chem. Phys.* **1985**, *89*, 2221.
- (9) (a) Gonzalez, C.; Schlegel, H. B. *J. Chem. Phys.* **1989**, *90*, 2154. (b) *J. Phys. Chem.* **1990**, *94*, 5523; (c) *J. Chem. Phys.* **1991**, *95*, 5853.
- (10) Hehre, W. J.; Ditchfield, R.; Pople, J. A. *J. Chem. Phys.* **1972**, *56*, 2257.
- (11) Schmidt, M. W.; Baldrige, K. K.; Boatz, J. A.; Elbert, S. T.; Gordon, M. S.; Jensen, J. H.; Koseki, S.; Matsunaga, N.; Nguyen, K. A.; Su, S.; Windus, T. L.; Dupuis, M.; Montgomery, J. A. *J. Comput. Chem.* **1993**, *14*, 1347.
- (12) (a) Anderson, K.; Malmqvist, P.-Å.; Roos, B. O. *J. Chem. Phys.* **1992**, *96*, 1218. (b) Anderson, K.; Malmqvist, P.-Å.; Roos, B. O. *J. Phys. Chem.* **1990**, *94*, 5483.
- (13) (a) Hariharan, P. C.; Pople, J. A. *Theor. Chim. Acta* **1973**, *28*, 213. (b) Krishnan, R.; Binkley, J. S.; Seeger, R.; Pople, J. A. *J. Chem. Phys.* **1980**, *72*, 650. (c) Frisch, M. J.; Pople, J. A.; Binkley, J. S. *J. Chem. Phys.* **1984**, *80*, 3265.
- (14) Anderson, K.; Blomberg, M. R. A.; Fülscher, M. P.; Kellö, V.; Lindh, R.; Malmqvist, P.-Å.; Noga, J.; Olsen, J.; Roos, B. O.; Sadlej, A. J.; Siegbahn, P. E. M.; Urban, M.; Widmark, P.-O. MOLCAS version 3, University of Lund, Sweden, 1994.
- (15) Chaban G. M.; Klimentko N. M.; Charkin O. P. *Struct. Prop. Mol.* (Transactions of Ivanovo Institute of Chemical Technology, Ivanovo) **1988**, 20–31.